論 文
49A-2-1

혼합형 전압안정도 해석

Hybrid Voltage Stability Analysis

金 原 謙* · 朱 雲 杓** · 金 建 中*** · 李 尙 中§
(Weon-Kyum Kim · Kern-Joong Kim · Oon-Pyo Zhu · Sang-Joong Lee)

Abstract - It is a complex process to analyze power system voltage stability problems with all of the dynamics of a system, because a large power network system sophisticatedly consists of generators, lines, loads and so forth. So we considered the dynamics of loads so as to analyze voltage stability problems in this paper. This paper presents a new analysis method -hybrid voltage stability method- by carrying out an analysis of steady state voltage stability and dynamic voltage stability simultaneously. To perform a steady state voltage stability program in advance makes it possible to cut down on laborious calculations so that an analysis of dynamic voltage stability becomes concise. The validity and efficiency of the method presented in this paper were verified by applying the IEEE 14 bus system

Key Words : Voltage Stability: Lagrangian Dual Function: Optimization, Dynamics of SVC, Induction Motor and OLTC: OOP

1. Introduction

Voltage instability is one of the challenging topics to prevent the powers system from collapsing. We can hardly expect to have a stable power supply in the near future unless the problem of voltage stability is resolved. It is an interesting contemporary worldwide topic. It is presently impossible to maintain voltage stability while applying the real time steady state control approach because of the dynamics of the power system in normal operation. However, the steady state approach is widely applied in spite of its deficiencies. When the power system is on-line operation with the approach, we should take into account the dynamics of the system. It is very difficult to analyze voltage stability of a large power system. Therefore we have developed an analysis method of dynamic voltage stability with load dynamic characteristics of the load buses, ignoring the dynamics of the generation buses, because the behavior of instability of phase angle could be maintained within a few seconds.

This paper presents the following. First it is well known that both long calculation time and a large storage memory in the computer are necessary to simulate dynamic problems such as a large power system voltage collapse with a relatively long time duration. To cope with this difficulty, after applying the steady state method in advance and then finding the weakest bus, we applied the dynamic voltage stability analysis method to the weakest one. Secondly, applying to the slip characteristics of the P-V curve and then analyzing the voltage stability, we propose an index method with which an operator can manage the operational margin. Thirdly, it is not only difficult but also extremely time consuming to either augment or develop new functions with an existing procedural and sequential programming language such as FORTRAN. To cope with this difficulty, we took advantages of an Object-Oriented Programming (OOP) language, which shortens the programming time and renders it more efficient when applied to modified cross-linked power system characteristics[1][2].

Fourthly, we proposed a steady state · dynamic load model consisting of reactive power controllers - On Load Tap Changers(OLTC), Static VAR Compensators (SVC) - and induction motors. The model embodies both non-linear equations and differential equations. To solve the differential equations, we introduced the fourth order Runge- Kutta numerical method[3].

2. Analysis of steady state voltage stability

The power equation is expressed by the multiplication

*正 會 員 : 東서울大 電氣工學科 講師 · 工博
**正 會 員 : 忠南大 電氣工學科 博士課程
***正 會 員 : 忠南大 電氣工學科 敎授 · 工博
§正 會 員 : 서울産業大 電氣工學科 專任講師 · 工博
接受日字 : 1999年 8月 14日
最終完了 : 2000年 1月 18日

of the bus voltage and current.

$$\dot{S}_{BUS} = \dot{V}_{BUS}\dot{I}^{*}_{BUS} \tag{1}$$

where bus voltage is a diagonal matrix such that;

$$[\dot{V}_{BUS}] = \begin{bmatrix} \dot{V}_1 & & 0 \\ & \ddots & \\ 0 & & \dot{V}_n \end{bmatrix}$$

The voltage can be described with a rectangular coordinate or polar coordinate. Putting X(a magnitude and a phase angle of the voltage) with respect to equation (1) because an interesting variable is a magnitude and a phase angle of the voltage, we define new two tensor such as equation (2) and equation (3);

$$\frac{\partial \dot{V}_i}{\partial X_i} = [e^{j\theta} \quad jV_i e^{j\theta}] = [\frac{1}{V_i} \quad j]^T V_i e^{j\theta} \triangleq \dot{T}_i \tag{2}$$

$$\frac{\partial \dot{V}_i^{*}}{\partial X_i} = [e^{-j\theta} \quad -jV_i e^{-j\theta}] = [\frac{1}{V_i} \quad -j]^T V_i e^{-j\theta} \triangleq \dot{T}_i^{*} \tag{3}$$

where X_i is vector such that $X_i = \begin{bmatrix} V_i \\ \theta_i \end{bmatrix}$

Constructing a Jacobian matrix with equation (2) and equation (3), we can express four cases in the following equations (4)~(7).

Case (i,i)

$$\begin{aligned} \frac{\partial \dot{S}_i}{\partial X_i} &= \frac{\partial \dot{S}_i}{\partial \dot{V}_i}\frac{\partial \dot{V}_i}{\partial X_i} + \frac{\partial \dot{S}_i}{\partial \dot{V}_i^{*}}\frac{\partial \dot{V}_i^{*}}{\partial X_i} \\ &= \dot{I}_i^{*}\dot{T}_i + \dot{V}_i\dot{y}_i^{*}\dot{T}_i^{*} + \dot{V}_i\dot{y}_{io}^{*}\dot{T}_i^{*} \end{aligned} \tag{4}$$

Case (i,k)

$$\frac{\partial \dot{S}_i}{\partial X_k} = \frac{\partial \dot{S}_i}{\partial \dot{V}_k^{*}}\frac{\partial \dot{V}_k^{*}}{\partial X_k} = -\dot{y}_{ik}^{*}\dot{V}_i\dot{T}_k^{*} \tag{5}$$

Case (k,i)

$$\frac{\partial \dot{S}_k}{\partial X_i} = \frac{\partial \dot{S}_k}{\partial \dot{V}_i^{*}}\frac{\partial \dot{V}_i^{*}}{\partial X_i} = -\dot{y}_{ki}^{*}\dot{V}_k\dot{T}_i^{*} \tag{6}$$

Case (k,k)

$$\begin{aligned} \frac{\partial \dot{S}_k}{\partial X_k} &= \frac{\partial \dot{S}_k}{\partial \dot{V}_k}\frac{\partial \dot{V}_k}{\partial X_k} + \frac{\partial \dot{S}_k}{\partial \dot{V}_k^{*}}\frac{\partial \dot{V}_k^{*}}{\partial X_k} \\ &= \dot{I}_k^{*}\dot{T}_k + \dot{V}_k\dot{y}_{ki}^{*}\dot{T}_k^{*} + \dot{V}_k\dot{y}_{ko}^{*}\dot{T}_k^{*} \end{aligned} \tag{7}$$

Equations (4) & equation (7) are diagonal Jacobian matrices and equation (5) & equation (6) off-diagonal matrices, which consist of sparsed matrices with 0 slots. The power mismatch equation is expressed in equation (8);

$$\begin{bmatrix} \Delta\dot{S}_1 \\ \Delta\dot{S}_2 \\ \vdots \\ \Delta\dot{S}_n \end{bmatrix} = [J] \begin{bmatrix} \Delta X_1 \\ \Delta X_2 \\ \vdots \\ \Delta X_n \end{bmatrix} \tag{8}$$

where, [J] is a defined Jacobian matrix with [2n x 2n] dimension in equation (9);

$$J \triangleq \begin{bmatrix} \frac{\partial \dot{S}_1}{\partial X_1} & \frac{\partial \dot{S}_1}{\partial X_2} & \cdots & \frac{\partial \dot{S}_1}{\partial X_n} \\ \frac{\partial \dot{S}_2}{\partial X_1} & \frac{\partial \dot{S}_2}{\partial X_2} & \cdots & \frac{\partial \dot{S}_2}{\partial X_n} \\ \vdots & \vdots & \ddots & \vdots \\ \frac{\partial \dot{S}_n}{\partial X_1} & \frac{\partial \dot{S}_n}{\partial X_2} & \cdots & \frac{\partial \dot{S}_n}{\partial X_n} \end{bmatrix} \tag{9}$$

Because it is understood that voltage instability is a problem of power loss mismatch, we have defined the power loss as an objective function with a power equation equality constraint, and formulated a problem such that equation (10);

$$\begin{aligned} &\text{Min } \dot{S}_{Loss} \\ &\text{s.t. } \dot{S}(X) = 0 \end{aligned} \tag{10}$$

Applying the Lagrangian dual function of the optimality technique to equation (10), we defined it in equation (11);

$$L \triangleq \dot{S}_{Loss} + \dot{\lambda}_S^T\dot{S}(X) \tag{11}$$

where the Lagrangian multiplier λ_P denotes the real power loss sensitivity with respect to the real power load change and λ_Q the reactive power loss sensitivity with respect to its reactive change and where $\dot{S}_{Loss}$ is a vector, and $\dot{\lambda}_S$ is a vector such as [2n x 1] dimension. where a derivative of the Lagrangian multiplier is expressed such that;

$$\dot{\lambda}_S = \begin{bmatrix} \lambda_P \\ \lambda_Q \end{bmatrix}$$

Defining a Lagrangian function, we formulated a constraint problem into an un-constrained one. The optimization problem of the dual Lagrangian function with un-constrained condition is expressed as;

$$\begin{aligned} \frac{\partial L}{\partial X} &= \frac{\dot{S}_{Loss}}{\partial X} + \frac{\dot{S}(X)}{\partial X}\dot{\lambda}_S \\ &= \frac{\dot{S}_{Loss}}{\partial X} + [J]^T[\ \dot{\lambda}_S\ ] = 0 \end{aligned} \tag{12}$$

$$\frac{\partial L}{\partial \lambda_S} = \dot{S}(X) = 0 \tag{13}$$

An index of steady state voltage stability with respect to the loss of power sensitivity is defined as;

$$[\ \dot{\lambda}_S\ ] = -[J]^{-T}\frac{\partial \dot{S}_{Loss}}{\partial X} \tag{14}$$

3. Analysis of dynamic voltage stability

The slip of an induction motor, which has an equilibrium point when the balance between an electrical input and a mechanical output is maintained is expressed as in equation (15) in the kth bus [5] ;

$$M\frac{d\omega}{dt} = (1-s_k)P_{ek} - P_{mk} \qquad (15)$$

where M is an angular moment denoted by $I\omega$ and s_k the slip at the kth bus. The slip is the ratio of the difference between the actual speed(ω) and the synchronous speed (ω_0) to the synchronous one such that ;

$$s=\frac{\omega_0-\omega}{\omega_0}$$

Substituting $\omega = \omega_o(1-s_k)$ into equation (15), we get the equation (16).

$$I_k(1-s_k)\omega_o\frac{d(1-s_k)\omega_o}{dt} = (1-s_k)P_{ek} - P_{mk} \qquad (16)$$

Therefore we get a differential equation with respect to induction motor slip such as equation (17);

$$\frac{ds_k}{dt}=\frac{1}{I_k\omega_0^2}\left(\frac{P_{mk}}{1-s_k}-P_{ek}\right) \qquad (17)$$

where I_k : inertia moment of induction motor
s_k : induction motor slip at the k^{th} bus
P_{mk} : mechanical output at the k^{th} bus
P_{ek} : electrical input at the k^{th} bus
$\omega_0=2\pi f_0$: angular velocity of system (f_o = 60 Hz)

A Static VAR Compensator(SVC) controls the bus voltage - the difference between a reference voltage and the load demand voltage in order to supply reactive power. The SVC supplies it to a network grid when the difference exists such as in equation (18) [6],[7];

$$\frac{dB_{SVC_k}}{dt}=\frac{1}{T_{SVC_k}}(V_{SREF}-V_D) \qquad (18)$$

where, B_{SVC_K} : Injection reactive power at the k^{th} bus.
T_{SVC_K} : Time constants of SVC at the k^{th} bus.
V_{SREF} : reference voltage of SVC

In addition, we should take into account that the SVC has a capacity to supply its reactive power range between an upper limit and lower limit. After getting the reactive power of SVC to inject, we confirm whether its value is within its limits; If its value is larger than the limits, we should have the injection power adjusted to its limits in order to reflect the SVC behavior.

An OLTC, which is a controller to maintain the reference bus voltage, is comparable to SVC and can be delineated with differential equation (19).

$$\frac{dn_k}{dt}=\frac{1}{T_{TAP_k}}(V_{TREF}-nV_D) \qquad (19)$$

where, n_k : Tap ratio of OLTC at the k^{th} tap
T_{TAP_k} : Time constant of OLTC at the k^{th} tap
V_{TREF} : Voltage reference of OLTC

Since the dynamics of generators are faster than those of voltage collapse we ignored the dynamics of generators. We concluded that one of the most efficient ways, to reflect the load dynamics with respect to voltage stability, is to include induction motor dynamics because induction motors are more widely used than other loads as mechanical power sources.

We proposed a voltage stability criteria after studying the induction motor load characteristics. Expressing the induction motor stability as a function of slip, by the fact of the cross point between load characteristic curve and supply characteristic curve, we divided it into two regions - a stable region and an unstable region. The stability characteristics with respect to induction motor slip are delineates with Fig 1, where V_D is a load voltage, P_e an electrical output, P_M a mechanical output, and P_D a load output.

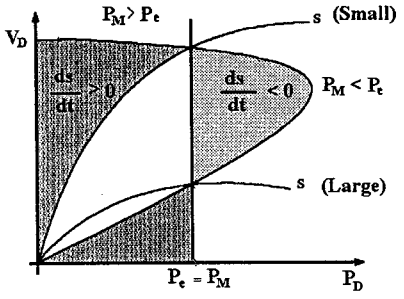

Fig. 1 P-V curve and slip dynamics of an induction motor

On the basis of an initial equilibrium point axis, the sign of change of slip is positive in the left side plane, and negative in the right one. If the existing slip in the right side of the equilibrium point increases, the slip in left plane decreases. The power from the load bus is determined according to the P-V nose curve in Fig 1. As

the slip increases in the area between the lower part of the P-V curve and a cross point with the slip curve, real power decreases. Examining the facts above, we get criteria for voltage stability such that;

$$① \frac{ds}{dt} > 0 \text{ AND } \frac{dP_D}{dt} > 0 \text{ Stable Solution(Upper Solution)} \tag{20}$$

$$② \frac{ds}{dt} < 0 \text{ AND } \frac{dP_D}{dt} > 0 \text{ Stable Solution(Upper solution)} \tag{21}$$

$$③ \frac{ds}{dt} > 0 \text{ AND } \frac{dP_D}{dt} < 0 \text{ Unstable Solution(Lower Solution)} \tag{22}$$

$$④ \frac{ds}{dt} < 0 \text{ AND } \frac{dP_D}{dt} < 0 \text{ Unstable Solution(Lower Solution)} \tag{23}$$

where "Stable Solution" means the stable solution for a calculation of load power flow.

In the case of equation (23), though the initial operation point remains in the unstable solution region, it can reach the stable region through the slip curve if the slip decreases.

However in the case of equation (22), the initial operation point remains in unstable solution region and follows through the slip curve with increasing slip in the unstable region.

Being satisfied with the condition in equation (24), we stop the iteration of calculation and get the break-point for the instability according to the criteria for voltage collapse.

$$\left\{ \frac{ds}{dt} > 0 \quad \text{AND} \quad \frac{dP_D}{dt} < 0 \right\} \text{ or } \left\{ \| \frac{ds}{dt} \| \leq \varepsilon \right\} \tag{24}$$

For equation (24) the calculation is complete when either the slip reaches an equilibrium point or slip increases in the unstable solution region.

4. Class Design of Load Flow

This study program consists of several classes as expressed in Fig 2. The major components are the load flow module and the voltage stability module. While load flow module and the voltage stability module are constructed separately, the load flow module shall be inherited from the voltage stability module.

An inheritance means that the new program or module receives the characteristics of an existing one and can apply them to other characteristics without modifying itself.

Being inherited from an original code, the program is prevented from accessing both the data and the code of the original one, and therefore needs capsulizing. After executing its function separately in advance and depending on control variables if necessary, the load flow calculation module in the program can execute its module. Meanwhile the structure of the data for the module is the same as that of the original load flow one.

While it is inevitable, when modifying the FORTRAN programming, to duplicate and clone the same structure of data in the program, we can overcome and execute its program with multi-inherent data after defining the data as a class having inherited characteristics.

Poly-morphism means that an operator or a function which has even same structure can execute a different operation depending on the situation. If an input-output structure of data is different from its original one, we sometimes have to encode all of the code from the beginning for an existing procedural programming.

However, in Object Oriented Programming, an operator of program can call and execute its defining function depending on the situation while overriding the existing operators .

Poly-morphism contributes to analyze a load flow problem when using the tensor technique. Tensor class has a [2 × 2] matrix data structure because we enable a user to express arbitrarily two complex values or four double values. The arrow in Fig 2 shows the inheritance relation.

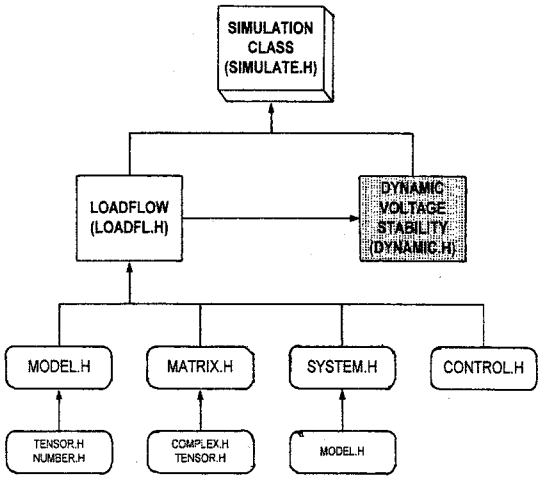

Fig. 2 Inheritance structure of Simulation class

Table 1 Classes used in the program

Name of Class	Contents of Class
SIMULATE	A class governing main program.
LOADFL	A main class of load flow calculation inheriting the voltage stability.
DYNAMIC	A class executing the dynamic stability
MODEL	A class managing the input- output of data and load format
MATRIX	A class managing and storing the sparse matrix data load format
SYSTEM	A class managing and storing the data of calculation
CONTROL	A class constructing the control variable
COMPLEX	A class defining the complex data format
TENSOR	A class defining and controlling two tensors

5. Case studies

5-1. Analysis of steady state voltage stability

Table 2 is a calculation result using the steady state voltage module after initial load flow calculating with the 14 bus network power system in Fig 3. The shaded slot in Table 2 shows a bus being calculated as the largest steady state voltage indicator(λ_Q) at the 14th bus. In Table 2, λ_P denotes a sensitivity of real power loss, λ_Q a sensitivity of reactive power loss, P_G a real generation power, P_D a real load power, Q_G a reactive generation power, and Q_D a reactive load power. Fig 4 delineates the voltage collapse index just before the voltage collapse when increasing the load constantly.

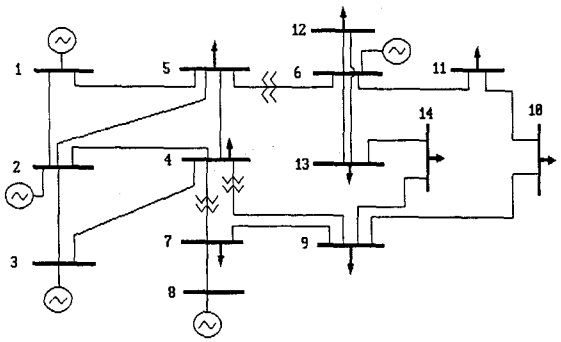

Fig. 3 IEEE 14 bus grid system

Table 2 Steady state voltage collapse index after initial load flow

No. of Bus	V	λ_P	λ_Q	P_G	P_D	Q_G	Q_L
1	1.06	-5.09e-57	1.393e-41	2.324	-0.16	0	0
2	1.045	0.06282	-2.082e-41	0.183	0	0.217	0.127
3	1.01	0.1339	2.264e-41	0	0.044	0.942	0.19
4	1.019	0.1123	0.006061	0	0	0.478	-0.039
5	1.02	0.09462	0.006742	0	0	0.076	0.016
6	1.07	0.0993	6.676e-42	0	0	0.112	0.075
7	1.062	0.1161	0.006062	0	0	0	0
8	1.09	0.1207	4.772e-42	0	0	0	0
9	1.056	0.1139	0.009778	0	0	0.295	0.166
10	1.051	0.1155	0.01392	0	0	0.09	0.058
11	1.057	0.1102	0.01003	0	0	0.035	0.018
12	1.055	0.1134	0.01174	0	0	0.061	0.016
13	1.05	0.1178	0.01696	0	0	0.135	0.058
14	1.036	0.1329	0.02883	0	0	0.149	0.05

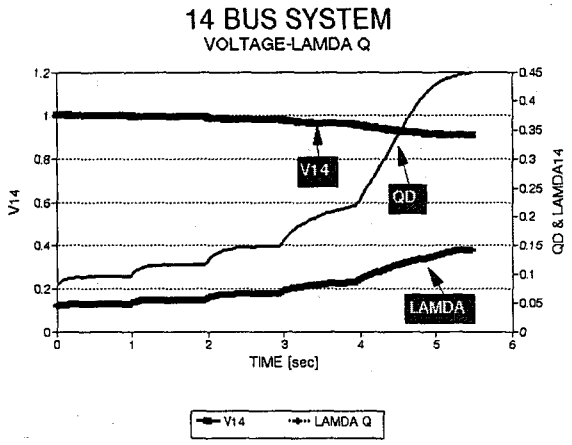

Fig. 4 Relationship between steady state voltage stability index and voltage of 14 bus

5-2. Analysis of dynamic voltage stability

Table 3 shows a result of four case studies with respect to the dynamic stability variables- initial slip, time step, end time, time control, load ratio of induction motor, power factor. We simulated the 14 bus system in the case of a disturbance, a mechanical output increase, and a contingency. In addition, when injecting the reactive power compensator SVC, we analyzed the status of the voltage recovery. In dynamic data, the load bus is presumed to have induction motor loads.

- Case 1) Normal operation
- Case 2) Disturbance
  - Case of increasing the mechanical output of the induction motor (power factor 95%)
- Case 3) Contingency
  - Case of increasing the mechanical output of the induction motor (one line fault)
- Case 4) Injection of the reactive power compensator
  - Case of injecting SVC

Table 3 Case study of 14 bus system [bus #14]

Condition / Case		Case 1	Case 2	Case3	Case4
초기슬립(ISLIP)		0.01	0.01	0.01	0.01
Time-Step [sec]		0.05	0.05	0.05	0.05
End-Time [sec]		1	1	1	1
Time control [sec]		20	20	20	20
Ratio of Induction Motor(IM load)		100%	100%	100%	100%
Power factor of IM		0.95	0.95	0.95	0.95
Increase of Mechanical Output [p.u]		0.0	0.1	0.1	0.1
Contingency	Duration	X	X	0.5 sec	X
	One line fault	X	X	6-13	X
SVC	Time constant	X	X	X	1.0 sec
	Duration of Injection	X	X	X	2 sec
	Power of Injection	X	X	X	0.5

Fig 5(case 1) shows the voltage and the slip of the induction motor at the 14th bus in normal operation both with the initial slip of induction motor and without disturbance. Fig 6 (case 2) shows the voltage and the slip of induction motor at the 14th bus with increasing mechanical output of the induction motor load.

We simulated the situation which increased mechanical output by 0.1 [p.u.] every 1 second until it reached the unstable point, when the induction load is 100% and its power factor is 95%. The curve of Fig 6 shows that the voltage decreases and the slip reaches to 1.0 at 7.1 seconds. We simulated the situation with one line fault at the 16th bus(the connection between the 6th line and the 13th) in the Case 2 condition.

The slip curve of case 3 shows that the slip is reaches 1.0 at 6.2 seconds, while it did 1.0 slip at 7.1 second in Case 2, when the voltage was being decreased. Fig 8(case 4) indicates that the voltage is restored and the capacity to supply the load power recovers from the lowered capacity of the case 2, when the SVC is operated at 2 seconds in Case 2. The slip curve of case 4 (Fig 8) shows that the slip reaches 1.0 at 7.8 seconds while it reaching 1.0 slip at 7.1 seconds in case 2 when the voltage was being decreased.

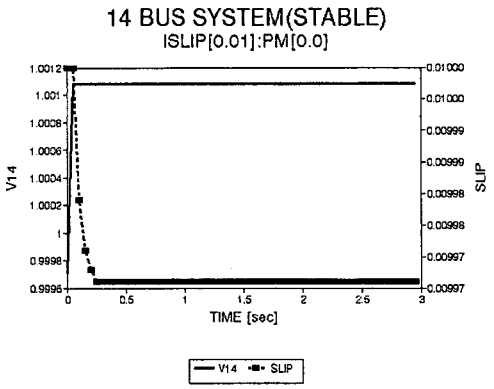

Fig. 5 Relationship between voltage and slip in the steady state case study

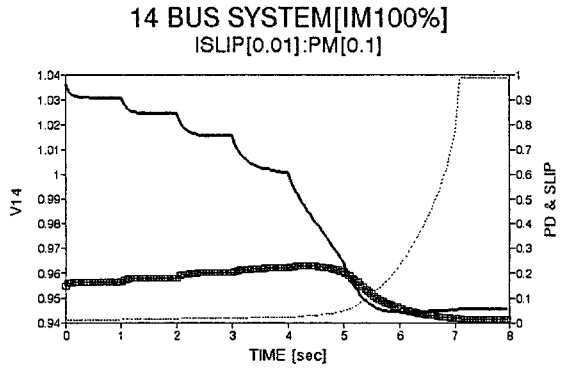

Fig. 6 Relationship between voltage and slip increasing IM mechanical power

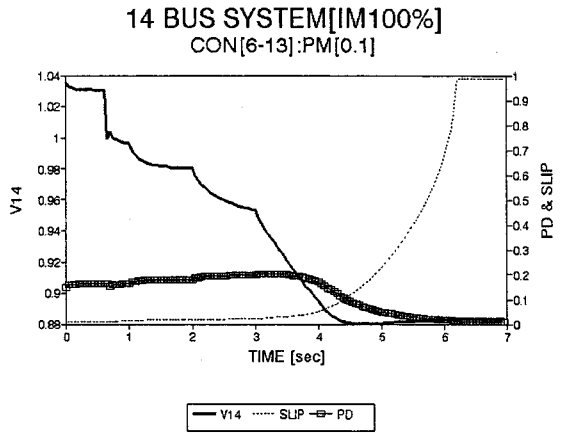

Fig. 7 Relationship between voltage and slip after line fault

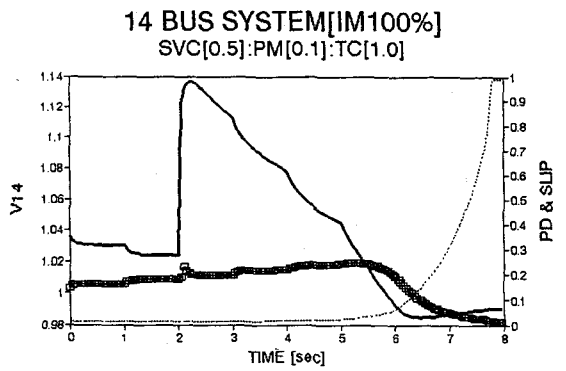

Fig. 8 Relationship between voltage and slip after SVC operation

6. Conclusion

This paper presents a new analysis method, as a way of distinguishing the degree of voltage instability - a criterion for voltage stability - and suggests an analysis method of steady state voltage stability and dynamic voltage stability simultaneously. The results of this paper are as follows;

1. It is a developed voltage instability criteria including load dynamics that we conclude from the facts, "the voltage becomes unstable if the slip of the induction motor increases monotonously and the load of active power decreases monotonously on the P-V nose curve." It was examined through the case study that the induction motor stalls when the slip of induction motor continues to increase and arrived at slip 1.0 .

2. The calculation time was reduced significantly and analyzing dynamic voltage stability time was shortened when we performed the steady state voltage stability program in advance, and then chose and applied the dynamic voltage stability one to the weakest bus.

3. The calculation of complex numbers was simplified when we applied the "poly-morphism of the operator", which is a characteristic of OOP, to the tensor method.

Hereafter we expect to develop a method, solving the voltage stability problem which covers the dynamic model of generation end buses in addition to that of load buses.

References

[1] I. Jacobson and M. Christerson," Object-Oriented Programming for Flexible Software Engineering", Addison-Wesly, pp. 43-69, 1992.

[2] J.H.Yu, "A Guide to OOP Borland C++", Jungbo-Munhwa Publishing, pp.15-51, 1992.

[3] E. Kreyszig, "Advanced Engineering Mathematics" 4th Edition, Vol I, Wiley, pp. 309-366, 1976.

[4] M.S.Bazaraa and C.M. Shetty," Nonlinear Programming Theory and Algorithms ", John Wiley & Sons ,Inc, pp.124-223, 1979.

[5] A. Yokoyama, Y. Sekine and H. Ohtsuki,"Reverse Action of On-Load Tap Changer in Association with Voltage Collapse", IEEE Trans. on Power Systems, Vol.6, No.1, pp. 300-306, Feb. 1991.

[6] C.C.Liu,"Analysis of Tap-Changer Dynamics and Construction of Voltage Stability Regions", IEEE Trans. on Circuit and Systems, Vol.36, No.4, pp.575-590, April 1989.

[7] K.J.Kim, W.K.Kim, J.B.Chu,"Analysis of Dynamic Voltage Stability Using Induction Motor Model", KIEE, 44-1-3, pp.15-20, 1995.

저 자 소 개

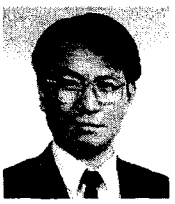

김 원 겸 (金 原 謙)

1961년 7월 5일생. 1984년 충남대 공대 전기공학과 졸업. 1987년 동 대학원 전기공학과 졸업(석사). 1996년 동 대학원 전기공학과 졸업(공박)

HP : 017-403-2490, FAX : 02-794-0807

E-mail : myloveyh@hitel.net

김 건 중 (金 建 中)

1953년 2월 12일생. 1975년 서울대 공대 전기공학과 졸업. 1977년 동 대학원 전기공학과 졸업(석사). 1985년 동 대학원 전기공학과 졸업(공박). 1977년 해군제2사관학교 교수. 현재 충남대 공대 전기공학과 교수

HP : 011-455-3247, FAX : 042-823-7970

E-mail : kjkim@ee.chungnam.ac.kr

주 운 표 (朱 雲 杓)

1956년 11월 3일생. 1984년 한양대 전기공학과 졸업. 1991년 충남대 전기공학과 석사 졸업. 1992년~현재 충남대 전기공학과 박사과정. 1988년~현재 한국원자력안전기술원 안전평가부 계측제어실 근무

TEL : 042-868-0249, FAX : 042-867-2535

E-mail : zhu@kins.re.kr

이 상 중 (李 尙 中)

1955년생. 1983년 성균관대 전기공학과 졸업. 1992.년 충남대 대학원 전기공학과 졸업(석사). 1995년 동대학 박사과정 졸업. 1998~현재 서울산업대 전기공학과 전임강사.

TEL : 02-936-1906

E-mail : sjlee@duck.snut.ac.kr